Tracer Additions for Spiraling Curve Characterization (TASCC): Quantifying stream nutrient uptake kinetics from ambient to saturation

Timothy P. Covino[1]*, Brian L. McGlynn[1], and Rebecca A. McNamara[1]
[1]Department of Land Resources and Environmental Sciences, Montana State University, Bozeman, Montana, USA

Abstract

Stream nutrient tracer additions and nutrient spiraling metrics are frequently used to quantify lotic ecosystem behavior. Of particular concern is the influence nutrient concentration exerts on nutrient retention and export. However, characterizing spiraling response curves across a range of concentrations has remained challenging, in part due to the large effort required to develop these curves using traditional (e.g., plateau or steady-state) approaches. Here we outline and demonstrate a new approach to quantify nutrient uptake kinetics from ambient to saturation using Tracer Additions for Spiraling Curve Characterization (TASCC). This approach provides a rapid and relatively easy technique for quantifying ambient-spiraling parameters, nutrient uptake kinetics and kinetic model parameterization, and assessment of stream proximity to saturation. We compare the results from TASCC to traditional breakthrough curve integrated and plateau approaches. We highlight the advantages of the TASCC approach for characterizing continuous spiraling response curves from ambient to saturation with a single tracer addition experiment, and its applicability to larger rivers where achieving plateau conditions (i.e., steady-state) is impractical.

In-stream processes have been implicated as important for watershed scale nitrogen (N) retention and export (Bernhardt et al. 2003). This area of research has expanded as N loading to terrestrial and aquatic ecosystems has increased (Vitousek et al. 1997; Turner and Rabalais 2003), and concerns over deleterious impacts on receiving water bodies have grown (Rabalais et al. 2009). Stream reach nutrient export is impacted by both biological (i.e., uptake) and physical (i.e., hydrologic loss) retention (Triska et al. 1989; Hart et al. 1992; Covino et al. 2010), and research has shown that in-stream uptake (i.e., biological retention) can be strongly influenced by nutrient concentration (Dodds et al. 2002; Earl et al. 2006; O'Brien et al. 2007). The relationship between biological uptake and nutrient concentration is of particular concern because nutrient uptake efficiency has been shown to decrease with elevated concentrations (Mulholland et al. 2002). However, characterizing these relationships within stream reaches has proven challenging. This is partially due to the large amount of time and effort needed to develop spiraling response curves using standard techniques (Stream Solute Workshop 1990; Earl et al. 2006). For these reasons, improved methods are needed to properly characterize stream reach spiraling-concentration relationships and help improve understanding of biological contributions to nutrient retention.

Concentrations, spiraling, and nutrient saturation—Understanding the influence nutrient concentration exerts on biological uptake kinetics has been central to stream nutrient spiraling research since at least the early 1990s (Mulholland et al. 1990; Hart et al. 1992). Stream nutrient spiraling describes the simultaneous hydrological (i.e., advection) and biological (i.e., uptake) processes that control downstream nutrient transport (Webster 1975; Wallace et al. 1977; Webster and Patten 1979).

As nutrients travel downstream, they spiral through water, particulate, and consumer compartments (Newbold et al. 1981). The average distance traveled during the completion of one spiral through these compartments is defined as the spiraling length (*S*, L) (Newbold et al. 1981). Total nutrient *S* is typically dominated by the average downstream distance traveled dissolved in the water column (Newbold et al. 1983), referred to as the uptake length (*S_w*, L) and Newbold (1981) further noted that shorter *S* indicates more efficient nutrient use relative to longer *S*.

Spiraling parameters, such as *S_w*, can be determined by measuring the downstream decline of biologically active tracer relative to conservative tracer during the plateau portion (i.e., steady-state, no change in concentration over time) of a constant-rate tracer experiment (which we refer to as the plateau approach, Stream Solute Workshop 1990). Both Mulholland et al. (1990) and Hart et al. (1992) found that *S_w* of phosphorous (P) lengthened with increased nutrient concentration. Mulholland et al. (1990) used plateau additions of radiotracer and unlabeled phosphate (PO_4^{-3}) to investigate relationships between uptake and concentration and found that both *S_w* and areal uptake rate (*U*, M×L^{-2}×T^{-1}) increased with elevated nutrient concentration. Furthermore, the authors noted that biological uptake became saturated at concentrations as low as 5 µg P L^{-1}. Hart et al. (1992) used unlabeled PO_4^{-3} plateau additions at three PO_4^{-3} concentrations and observed increases in *S_w* and *U* at elevated nutrient concentration, and found a linear relationship between concentration and *U*. However, the paucity of data (three point regression) makes drawing conclusions regarding uptake kinetics challenging. Mulholland et al. (2002) compared stable isotope ammonium ($^{15}NH_4$) and unlabeled (NH_4) plateau additions, and found that *S_w* lengthened with elevated nutrient concentrations. Together these results demonstrate that nutrient use efficiency, for both N and P, decreases with elevated nutrient concentrations, which has important implications for the downstream transport of nutrients, and suggests that biological retention may be lowest at times of highest nutrient export (Royer et al. 2004).

Because *S_w* is strongly influenced by stream discharge, biological uptake kinetics can more clearly be observed from analysis of relationships between concentration and uptake velocity (*V_f*, L×T^{-1}) and *U*, which partially account for hydrologic influences on *S_w*. *V_f* indicates nutrient uptake efficiency relative to nutrient availability and *U* represents the areal uptake of nutrient on a per area per time basis (Stream Solute Workshop 1990). Dodds et al. (2002) used plateau additions of ^{15}N and unlabeled N and found that *U* increased as stream concentration increased within stream reaches. The authors conducted plateau N additions at four concentrations, and used the regression between concentration and *U* to estimate uptake under conditions not influenced by nutrient additions (i.e., ambient uptake, *U_{amb}*). They further noted that linear extrapolation to *U_{amb}* using the origin and a single *U* value obtained

from one nutrient addition experiment will generally underestimate *U_{amb}* if the *U*-concentration relationship follows saturation kinetics (e.g., Michaelis-Menten kinetics, M-M). Earl et al. (2006) applied a novel approach where ^{15}N and unlabeled N were co-injected as constant-rate releases to investigate the influence of N concentration on spiraling within stream reaches at two to four manipulated nutrient levels (i.e., nutrient concentration controlled by addition of unlabeled N). The authors used this approach to determine stream reach uptake kinetics and to assign saturation response types (SRTs), which reflect stream reach proximities to saturated conditions. However, while the work of Earl et al. (2006) provided a large contribution to understanding concentration influences on nutrient spiraling, these analyses relied on scant data (2–4 points) to constrain relationships, which has been noted as problematic in previous research (e.g., Dodds et al., 2002). Accordingly, greater data density should constrain regressions and provide improved estimates of ambient spiraling metrics. Accomplishing this without the use of isotopic tracers is desirable given the high cost associated with stable isotope (e.g., ^{15}N) experiments and health concerns of using radiotracers (e.g., ^{32}P).

It is important to note that the typical approach applied during an unlabeled nutrient addition experiment addresses uptake of the added nutrient, not total nutrient uptake. Specifically, total uptake during a nutrient addition experiment is equal to the sum of ambient (i.e., uptake of background nutrient) and added nutrient uptake. In this paper, we refer to these spiraling metrics as ambient (i.e., uptake of background nutrient without the influence of added nutrient), added nutrient, and total nutrient uptake (i.e., the sum of ambient and added nutrient uptake during a nutrient addition experiment). Furthermore, we present and discuss how the Tracer Additions for Spiraling Curve Characterization (TASCC) approach accounts for both of these contributions (ambient and added nutrient) and quantifies total uptake through the use of nutrient addition experiments.

Tracer addition designs, TASCC, and response curves—A common theme among all of the aforementioned research is the plateau approach (i.e., constant-rate additions). This is a relatively time-consuming method for developing uptake-concentration relationships (i.e., spiraling response curves), because each constant-rate experiment produces only one spiraling metric for one concentration. For this reason, many of these studies have relied on few data points to analyze spiraling-concentration relationships. Inadequate characterization of uptake-concentration kinetics is problematic because it leads to incorrect nutrient export estimates (Mulholland et al. 2008) and poorly constrained extrapolations to higher or lower concentration behavior (Dodds et al. 2002). We suggest that methods for improved characterization of the relationships between *S_w*, *V_f*, *U* and nutrient concentration are needed to improve export models, constrain spiraling-concentration extrapolations (e.g., extrapolations to *U_{amb}*), to assess stream saturation state, and to increase basic understanding of stream nutrient spiraling dynamics.

Here, we outline and apply our newly developed TASCC approach to investigate the relationship between in-stream nutrient spiraling metrics and nutrient concentration. As opposed to relying on the plateau approach, TASCC capitalizes on the wide concentration range experienced by a stream reach across the breakthrough curve (BTC) of an instantaneous nutrient addition (i.e., slug). This approach provides a rapid and relatively easy method for quantifying uptake kinetics across a broad range of concentrations and assigning appropriate kinetic models (e.g., M-M, efficiency loss, first-order). In contrast to traditional slug methods (e.g., Tank et al. 2008), which produce only a single integrated spiraling metric for the entire BTC (hereafter referred to as the BTC-integrated approach), the TASCC method allows for characterization of continuous spiraling curves (i.e., high data density) across a wide range of concentrations from a single nutrient addition experiment. We compare the results of TASCC with results from BTC-integrated (e.g., Ruggiero et al. 2006; Tank et al. 2008), and standard plateau approaches to measuring spiraling over the same stream reaches during the same time period. Our results indicate good agreement between TASCC, BTC-integrated, and plateau approaches. However, we highlight the advantages of TASCC for fully and rapidly characterizing the relationships between S_w, V_f, U and nutrient concentration. We suggest that TASCC is an efficient and cost effective tool that offers 1) improved confidence in estimates of ambient-spiraling metrics determined from nutrient addition experiments; 2) enhanced characterization of spiraling response curves and parameterization of kinetic models; 3) accordingly better assessment of stream saturation state and inter-system comparison; and 4) applicability to large river systems where obtaining constant-rate plateau conditions is impractical.

Materials and procedures

Site description—We performed conservative (chloride, Cl) and biologically active (nitrate-nitrogen, NO_3-N) tracer addition experiments in two stream reaches (Middle Fork and Beehive) within the West Fork of the Gallatin River Watershed in the northern Rocky Mountains of southwestern Montana. The West Fork Watershed (212 km^2) is characterized by shallow soils and well-defined steep topography, with elevation across the drainage ranging between ~1800–3400 m. Average annual precipitation is less than 50 cm near the watershed outlet and exceeds 127 cm in the upper elevations, with 60% of precipitation falling during the spring and winter months (Lone Mountain NRCS SNOTEL #590, 2707 m elevation). The West Fork Watershed experiences a short growing season beginning in mid-June and ending in mid-September (McNab 1996). See Gardner and McGlynn (2009) for background water quality and additional watershed information.

The Middle Fork site is a third-order valley bottom stream approximately three km upstream from the confluence of the West Fork and the main stem of the Gallatin River. Geology is dominated by colluvial and glacial gravel deposits and vegetation consists of native grasses, shrubs, and willows (*Salix* spp.) in the riparian areas. Discharge (Q, L^3×T^{-1}) at Middle Fork ranges from 2.5 m^3 sec^{-1} during snowmelt driven peak flow, to 0.2 m^3 s^{-1} during baseflow. The average channel slope across the 1300 m Middle Fork stream reach was 1.01%, and environmental conditions during experiments at both sites are detailed in Table 1.

The Beehive site is a second-order stream closer to the headwaters with high elevation mountain topography comprised of granitic gneiss and gravel deposits. Beehive local vegetation consists of coniferous forest (Lodgepole pine [*Pinus contorta*], Blue spruce [*Picea pungens*], Engelmann spruce [*Picea engelmannii*], and Douglas fir [*Pseudotsuga menziesii*]) in the uplands and native grasses, willows (*Salix* spp.) and aspen (*Populus tremuloides*) groves in the riparian areas. Q at Beehive ranges between 0.2 m^3 s^{-1} during snowmelt driven peak flow, and 0.03 m^3 s^{-1} at baseflow, and the average channel slope along the 590 m study reach was 1.7%.

Experimental design—We performed tracer addition experiments in Middle Fork and Beehive in August 2007 and July 2008 to capitalize on spatial and temporal variation in hydraulics and N concentrations. We executed both plateau and slug releases at each site, and included a low and high NO_3-N plateau release at Beehive (Table 1). We compare and contrast various approaches to quantifying stream nutrient spiraling using these experiments as case studies. Furthermore, these two data-sets bracket the range of goodness of fit we observed across 12 stream reaches where experiments occurred. On each stream reach, we measured nutrient spiraling using plateau and slug nutrient additions. Prior to all experiments, we collected back-

Table 1. Stream characteristics for Beehive and Middle Fork sites on the dates we performed tracer additions.

Site	Date	Watershed area (km^2)	Downstream Q (m^3 s^{-1})	Median flow velocity (m s^{-1})	Distance (m)	Width (m)	Stream temperature (°C)	[NO_3-N$_{amb}$] (µg L^{-1})
Beehive*	29-Jul-08	5.7	0.137	0.342	590	2.7	7.9–12.4	2
Beehive-low [N]	30-Jul-08	5.7	0.121	0.329	590	2.7	7.0–10.9	2
Beehive-high [N]	30-Jul-08	5.7	0.121	0.329	590	2.7	7.0–10.9	2
Middle Fork*	22-Aug-07	83.4	0.207	0.210	1300	7.0	11.5–15.3	43
Middle Fork	23-Aug-07	83.4	0.199	0.205	1300	7.0	9.3–13.8	43

*Indicates a slug addition

ground (i.e., ambient) NO_3-N and Cl samples and measured stream width and depth at 12 evenly spaced sampling transects along the 590 m (Beehive) and 1300 m (Middle Fork) stream reaches. For each of these experiments, we measured Q at the downstream (base) and upstream (head) ends of the study reach. During plateau experiments, we released a solution of biologically active (potassium nitrate, KNO_3) and conservative (sodium chloride, NaCl) tracers (dissolved in stream water) to the head of the reach at a constant-rate. The solution was added at a location that ensured complete mixing before the tracer arrived at the first downstream sampling location. We measured stream conductivity in real time (2-s interval) at the base of the reach with a Campbell Scientific CS547A temperature and conductivity probe connected to a Campbell CR1000 data logger to determine when downstream plateau was achieved (i.e., no change in conductivity over time). During plateau conditions, we collected NO_3-N and Cl samples along the study reach at the 12 transects, moving upstream from downstream. For slug additions, we released a solution of KNO_3 and NaCl dissolved in stream water to the head of the study reach as an instantaneous addition (Fig. 1). At the base of the reach, we measured conductivity real time to determine when to collect samples across the slug profile. The change in tracer concentration over time at a downstream location is referred to as the tracer breakthrough curve (BTC), and we collected grab samples across the full range of the NO_3-N and Cl BTCs at the base of the reach (Fig. 1). We analyzed the slug BTC data using both BTC-integrated and dynamic TASCC approaches. With the traditional slug BTC-integrated approach (e.g., Ruggiero et al. 2006; Tank et al. 2008),

the amount of tracer recovered is determined through integration of the tracer BTCs to calculate one suite of spiraling metrics (e.g., single S_w, V_f, and U value) from each slug addition. Conversely, the dynamic TASCC approach calculates a distribution of spiraling metric values as a function of nutrient concentration for each tracer addition. Within the dynamic TASCC method, we calculated this distribution of values using a longitudinal uptake rate (k_w) and a mass-balance approach, and we compare the results obtained from these two methods. The k_w approach assumes an exponential decline of nutrient concentration with distance downstream, whereas the mass-balance approach makes no assumptions regarding the longitudinal change in concentration and instead calculates spiraling metrics using the difference between upstream added and downstream recovered nutrient mass.

As previously noted, nutrient spiraling measured during a typical nutrient addition experiment (whether plateau or slug) does not represent total nutrient uptake (i.e., U_{tot}), but rather the uptake of added nutrient (i.e., U_{add}). Therefore, U_{tot} is equal to the sum of ambient uptake (i.e., U_{amb}) and U_{add}, all of which (U_{amb}, U_{add}, and U_{tot}) we quantify using our new technique (TASCC). From U_{tot} versus nutrient concentration curves we determine stream uptake kinetics, fit kinetic models to these data, and quantify kinetic model parameters (e.g., M-M model parameters U_{max} and K_m). Application of TASCC requires accurate assessment of stream Q, reach morphology, and tracer concentrations. Detailed explanations of the steps required to complete each of the above-mentioned analyses are contained in the following sections.
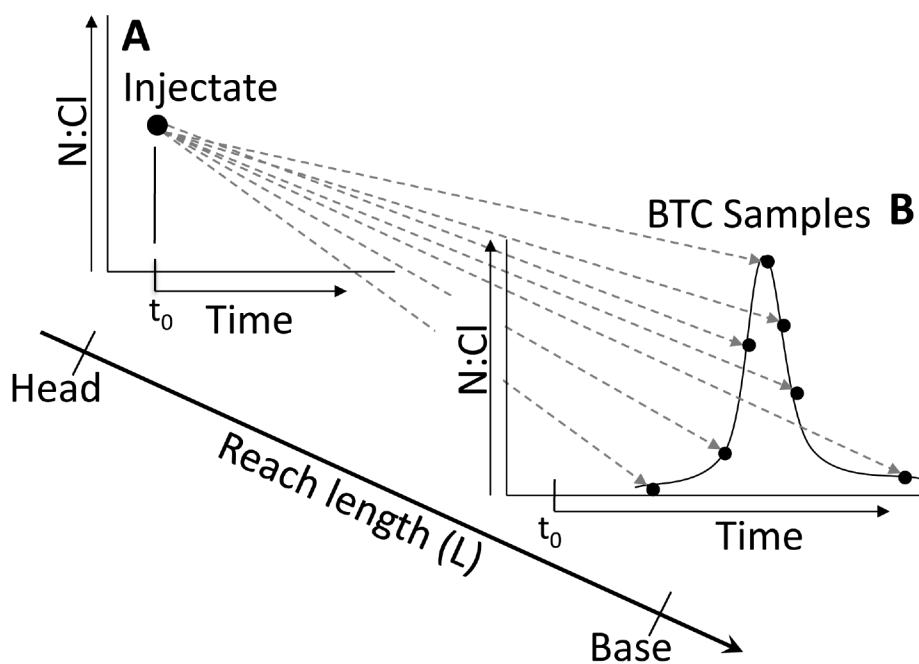

Fig. 1. Conceptual diagram illustrating the instantaneous (slug) release of conservative and biologically active tracers at (A) the head of a stream reach and tracer breakthrough curve (BTC) sampling at (B) the base of the reach. The grab samples collected at the base of the reach can be used to calculate BTC-integrated or dynamic TASCC spiraling parameters.

Stream discharge—A few hours before all of our stream nutrient addition experiments, we measured Q at the downstream and upstream endpoints of each experimental stream reach (Table 1). We used NaCl dilution gauging (Barbagelata 1928), and began at the base and moved to the head of the stream reach. We released NaCl as an instantaneous addition only far enough upstream of our sampling location (either the stream base or head) to allow for complete mixing (35–75 m), and determined appropriate mixing lengths by visual observation of complete mixing of fluorescent Rhodamine dye (RWT) immediately preceding our NaCl addition. We measured stream water specific conductance (SC) in real time with Campbell (Campbell Scientific) CS547A temperature and conductivity probes connected to Campbell CR1000 data loggers, logging at 2-s intervals. We developed a relationship between SC and NaCl concentration ($r^2 = 0.999$, $P < 0.0001$), and from this relationship, we calculated stream discharge (e.g., Payn et al. 2009). This approach provides independent site-specific measures of Q at the head and base of the study reach.

Estimating spiraling metrics from plateau additions of conservative and biologically active tracers—We dissolved conservative (NaCl) and biologically active nutrient tracers (KNO$_3$) in a carboy with stream water and released the solution into study streams (Beehive and Middle Fork) as plateau (i.e., constant-rate) additions. We used a Fluid Metering pump (Fluid Metering) to release the solution and measured the downstream change in stream water SC (logging equipment described above, two-second interval) at the base of the reach (590 m downstream at Beehive, 1300 m downstream at Middle Fork). SC values were used to determine when tracer in the stream reached plateau concentrations (i.e., no change in SC over time). During the plateau portion of the release, we sampled water for NO$_3$-N and Cl at the 12 transects along the study reach, moving upstream toward the injection location. These locations were always sampled prior to tracer addition experiments to determine ambient NO$_3$-N and Cl concentrations (i.e., background) in order to background correct plateau samples. All grab samples were placed on ice and returned to the lab the same day of the experiment, filtered through 0.4 µm Isopore membrane filters (Millipore), and frozen until analysis. Samples were analyzed for Cl and NO$_3$-N on an ion chromatograph (Metrohm Peak) with A-supp analytical and guard columns and a 200-µL injection loop.

Plateau approach for estimating spiraling metrics—Nutrient uptake length (S_w) can be estimated by measuring the longitudinal decline of biologically active tracer (nutrient) relative to conservative tracer with distance downstream during the plateau portion of a constant-rate tracer addition experiment (Stream Solute Workshop 1990). We plotted the natural log of background corrected NO$_3$-N:Cl of longitudinal grab samples collected during plateau conditions against distance downstream from the injection site. The slope of the line derived from these data is the plateau approach longitudinal uptake rate of added nutrient ($k_{w\text{-}add\text{-}plat}$). The plateau approach uptake length of added nutrient ($S_{w\text{-}add\text{-}plat}$) is calculated as the negative inverse of $k_{w\text{-}add\text{-}plat}$ (Eq. 1):

$$S_{w\text{-}add\text{-}plat} = -1/k_{w\text{-}add\text{-}plat} \qquad (1)$$

where $S_{w\text{-}add\text{-}plat}$ is uptake length (L), and $k_{w\text{-}add\text{-}plat}$ is the longitudinal uptake rate (L^{-1}). We also calculated plateau approach added nutrient areal uptake rates ($U_{add\text{-}plat}$) and uptake velocities ($V_{f\text{-}add\text{-}plat}$) using (Eqs. 2 and 3):

$$U_{add\text{-}plat} = Q \times [NO_3\text{-}N_{add\text{-}plat}]/S_{w\text{-}add\text{-}plat} \times w \qquad (2)$$

$$V_{f\text{-}add\text{-}plat} = U_{add\text{-}plat}/[NO_3\text{-}N_{add\text{-}plat}] \qquad (3)$$

where $U_{add\text{-}plat}$ is the plateau approach areal uptake rate of added nutrient (M×L^{-2}×T^{-1}), Q is stream discharge (L^3×T^{-1}), $[NO_3\text{-}N_{add\text{-}plat}]$ is the geometric mean of background corrected NO$_3$-N concentrations of longitudinal grab samples collected across the stream reach during constant-rate plateau conditions (M×L^{-3}), w is average wetted stream width measured across the stream reach (L), and $V_{f\text{-}add\text{-}plat}$ is the plateau approach uptake velocity (L×T^{-1}). The geometric mean reflects the magnitude of exposure experienced along a stream reach when an exponential decline in tracer concentration (i.e., longitudinal uptake rate) is assumed and is used for concentration calculations throughout this paper.

Estimating spiraling metrics from instantaneous slug additions of conservative and biologically-active tracers—In addition to constant-rate plateau additions, we also used instantaneous slug additions of conservative (Cl) and biologically active (NO$_3$-N) tracers to estimate nutrient spiraling parameters. We dissolved NaCl and KNO$_3$ with stream water in a carboy and released the solution to the stream as an instantaneous slug. We added 607 g Cl and 13.9 g NO$_3$-N at Beehive, and 1821 g Cl and 277.1 g NO$_3$-N at Middle Fork. We monitored SC BTCs real time at the base of the reach as in the constant-rate experiments at 2-s intervals. We used SC BTCs monitored real time to guide the collection of grab samples at the base of the reach to ensure characterization of the entire NO$_3$-N and Cl BTCs ($n = 14–21$ grab samples per release). Grab samples were collected on 45 s–4 min intervals at Beehive, and 1–10 min intervals at Middle Fork with more intense sampling occurring when concentration was more dynamic (i.e., changing quickly). Grab samples were placed on ice and returned to the lab the same day as the experiment, and treated and analyzed using the same methods described earlier. Grab samples collected before the experiment along the stream reach were used to background correct the slug addition grab samples.

Slug BTC-integrated approach for estimating spiraling metrics—For each instantaneous slug addition, we determined the amount of tracer (Cl and NO$_3$-N) added at the head that was recovered at the base of the stream reach. Tracer mass recovery (T_{MR}) was calculated as the product of Q and the time-integrated tracer concentration measured at the base of the stream reach (Eq. 4):

$$T_{MR} = Q \int_0^t T_C(t)\, dt \tag{4}$$

where T_{MR} is the tracer mass recovery (M), and T_C is the time-integrated tracer concentrations ($M \times T \times L^{-3}$) of background corrected Cl and NO_3-N. From the Cl and NO_3-N T_{MR} values, we calculated the BTC-integrated uptake length of added nutrient ($S_{w-add-int}$). $S_{w-add-int}$ was calculated by plotting the natural log of the injectate NO_3-N:Cl ratio and the BTC-integrated NO_3-N:Cl [i.e., $T_{MR}(NO_3$-N):$T_{MR}(Cl)$] ratio against stream distance, similar to the approaches used by Ruggiero et al. (2006) and Tank et al. (2008). The slope of the line derived from these data is the BTC-integrated longitudinal uptake rate of added nutrient ($k_{w-add-int}$), and $S_{w-add-int}$ is the negative inverse of $k_{w-add-int}$. In the examples given here, we are using only the head and the base of the reach to calculate these parameters; however, this approach will also work using numerous points (i.e., additional sampling locations) along a stream reach (e.g., Covino et al. 2010). We calculated BTC-integrated added nutrient areal uptake rates ($U_{add-int}$) and uptake velocities ($V_{f-add-int}$) using Eqs. 5 and 6:

$$U_{add-int} = Q \times [NO_3\text{-}N_{add-int}]/S_{w-add-int} \times w \tag{5}$$

$$V_{f-add-int} = U_{add-int}/[NO_3\text{-} N_{add-int}] \tag{6}$$

where $U_{add-int}$ is the BTC-integrated areal uptake rate of added nutrient ($M \times L^{-2} \times T^{-1}$), $[NO_3\text{-}N_{add-int}]$ is the geometric mean of observed and conservative BTC-integrated NO_3-N concentrations ($M \times L^{-3}$), and $V_{f-add-int}$ is the BTC-integrated uptake velocity of added nutrient ($L \times T^{-1}$). The geometric mean of observed and conservative BTC-integrated NO_3-N concentrations was calculated as Eq. 7:

$$[NO_3\text{-}N_{add-int}] = \sqrt{\frac{Q \int_0^t [NO_3\text{-}N_{add-obs}](t)\,dt}{\int_0^t Q(t)\,dt} * \frac{Q \int_0^t [NO_3\text{-}N_{cons}](t)\,dt}{\int_0^t Q(t)\,dt}} \tag{7}$$

where $[NO_3\text{-}N_{add-obs}]$ is the background corrected NO_3-N concentrations in the grab samples collected across the slug BTC (i.e., concentration of added NO_3-N), and $[NO_3\text{-}N_{cons}]$ is the conservative NO_3-N concentrations for the grab samples collected across the slug BTC. We define conservative NO_3-N as the amount of NO_3-N that would be transported to a sampling site if NO_3-N traveled conservatively (i.e., no uptake, the maximum that could arrive at a site), and N_{cons} was calculated as the product of observed Cl concentration (background corrected) and the N:Cl of the injectate solution. We used the geometric mean of conservative and observed NO_3-N concentration because it provides a good approximation of the NO_3-N concentration experienced across the stream reach of study.

Dynamic TASCC approach for estimating spiraling metrics—We developed a new technique (TASCC) to investigate the influ-

ence stream NO_3-N concentration has on nutrient spiraling parameters and to rapidly determine stream nutrient uptake kinetics using slug additions. We calculated added nutrient dynamic longitudinal uptake rates ($k_{w-add-dyn}$) for each grab sample by plotting the natural log of the NO_3-N:Cl ratio of injectate and each grab sample (background corrected) collected at the base of the reach against stream distance (Fig. 2). The respective slopes of the lines derived from these data pairs are the $k_{w-add-dyn}$ values for each grab sample. $S_{w-add-dyn}$ metrics are then calculated as the negative inverse of the $k_{w-add-dyn}$ values (Fig. 2).

We applied the TASCC approach to calculate dynamic areal uptake rates ($U_{add-dyn}$) and uptake velocities ($V_{f-add-dyn}$) of added nutrient from our instantaneous slug addition experiments. With the dynamic approach we estimate uptake parameters for each grab sample across the BTC, as opposed to developing one integrated metric as in the BTC-integrated approach. For each grab sample across the BTCs, we calculated $U_{add-dyn}$ using Eq. 8:

$$U_{add-dyn} = Q \times [NO_3\text{-}N_{add-dyn}]/S_{w-add-dyn} \times w \tag{8}$$

where $U_{add-dyn}$ is the dynamic areal uptake rate of added nutrient ($M \times L^{-2} \times T^{-1}$) for each grab sample, and $[NO_3\text{-}N_{add-dyn}]$ is the geometric mean of observed and conservative NO_3-N concentration ($M \times L^{-3}$) in the grab sample of interest. $[NO_3\text{-}N_{add-dyn}]$ was calculated for each grab sample (not integrated as above in the BTC-integrated calculations) as Eq. 9:

$$[NO_3\text{-}N_{add-dyn}] = \sqrt{[NO_3\text{-}N_{add-obs}] * [NO_3\text{-}N_{cons}]} \tag{9}$$

where $[NO_3\text{-}N_{add-obs}]$ is the background corrected NO_3-N concentration ($M \times L^{-3}$) observed in a grab sample, and $[NO_3\text{-}N_{cons}]$ is the background corrected NO_3-N concentration expected in the grab sample if added NO_3-N traveled conservatively (i.e., no uptake, the maximum that could arrive at a site). From $U_{add-dyn}$, we calculated $V_{f-add-dyn}$ (Eq. 10).

$$V_{f-add-dyn} = U_{add-dyn}/[NO_3\text{-}N_{add-dyn}] \tag{10}$$

TASCC mass-balance approach for estimating spiraling metrics—In addition to the approach described above that uses a longitudinal exponential decline model (i.e., $k_{w-add-dyn}$) to calculate spiraling parameters, we also developed a mass balance approach to calculate dynamic areal uptake rate ($U_{add-dyn-MB}$) from the difference between conservative NO_3-N and observed NO_3-N associated with each sample taken across tracer BTCs (Eq. 11).

$$U_{add-dyn-MB} = ([NO_3\text{-}N_{cons}] - [NO_3\text{-}N_{add-obs}]) \times Q/streambed\ area \tag{11}$$

where *streambed area* is the bed area across the stream reach and is calculated as the product of average wetted width (L)
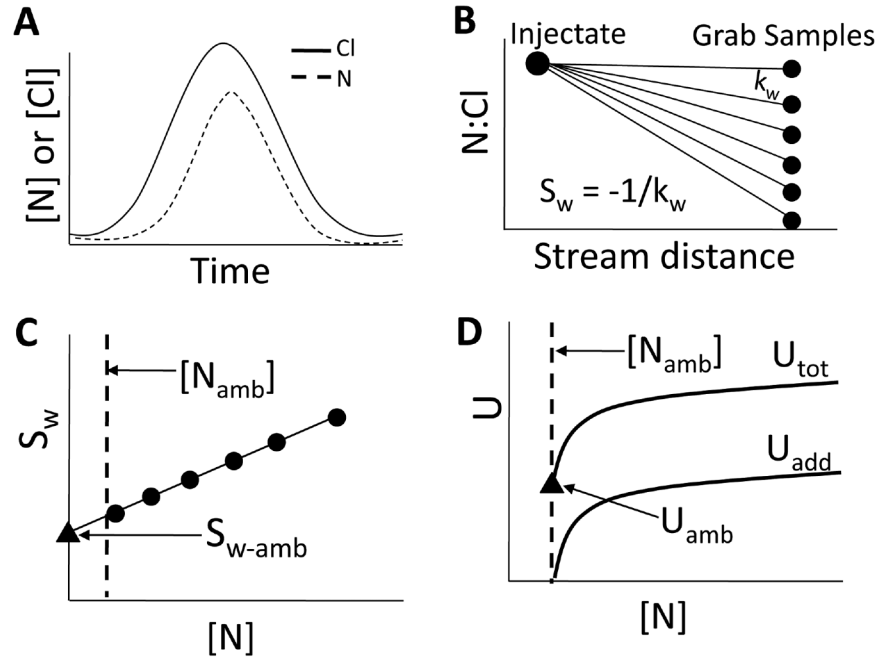
Fig. 2. Conceptual diagram illustrating the TASCC approach. (A) Sample the Cl and NO_3-N BTCs across the full range of concentrations at the base of the reach. (B) Calculate added nutrient dynamic longitudinal uptake rates ($k_{w\text{-}add\text{-}dyn}$) for each grab sample by regressing the natural log of the NO_3-N:Cl ratio of injectate and each grab sample against stream distance. (C) Calculate added nutrient dynamic uptake lengths ($S_{w\text{-}add\text{-}dyn}$) for each grab sample as the negative inverse of $k_{w\text{-}add\text{-}dyn}$, plot the $S_{w\text{-}add\text{-}dyn}$ values against total dynamic nutrient concentration, and extrapolate the regression to estimate ambient uptake length ($S_{w\text{-}amb}$). (D) Convert $S_{w\text{-}amb}$ to ambient areal uptake (U_{amb}) and uptake velocity ($V_{f\text{-}amb}$) for each grab sample, combine added nutrient uptake (U_{add}) with U_{amb} to yield total uptake (U_{tot}) for each grab sample, plot U_{tot} metrics against total dynamic nutrient concentration, and fit appropriate kinetic models.

and stream distance (L). This approach allows for a simple mass-balance calculation of U that assumes nothing about the longitudinal change in concentration along the stream reach. However, V_f and S_w can be back calculated from $U_{add\text{-}dyn\text{-}MB}$ values if an exponential model is assumed in the back-calculation.

Variable travel time approach for estimating spiraling metrics—To address differential tracer velocities on the rising and falling limbs of the BTCs, we include a derivation of time-dependent uptake metrics. Accordingly, we calculated added nutrient dynamic areal uptake rates and uptake velocities using variable travel times across the BTCs ($U_{add\text{-}dyn\text{-}TT}$ and $V_{f\text{-}add\text{-}dyn\text{-}TT}$) using Eqs. 12 and 13:

$$U_{add\text{-}dyn\text{-}TT} = z \times (L/TT) \times [NO_3\text{-}N_{add\text{-}dyn}]/S_{w\text{-}add\text{-}dyn} \qquad (12)$$

$$V_{f\text{-}add\text{-}dyn\text{-}TT} = U_{add\text{-}dyn\text{-}TT}/[NO_3\text{-}N_{add\text{-}dyn}] \qquad (13)$$

where $U_{add\text{-}dyn\text{-}TT}$ is the added nutrient areal uptake calculated using the variable travel time approach, z is average wetted stream depth (L), L is the stream reach length, TT is the time from tracer addition to sample collection which is analogous to a time of stream system exposure for the added tracers, and $V_{f\text{-}add\text{-}dyn\text{-}TT}$ is the added nutrient uptake velocity calculated using the variable travel time approach.

Using dynamic spiraling to estimate ambient stream spiraling parameters—We used our measured $S_{w\text{-}add\text{-}dyn}$ versus stream NO_3-N concentration data to determine the impact stream NO_3-N

concentration had on $S_{w\text{-}add\text{-}dyn}$, and to estimate $S_{w\text{-}amb}$ for the study reaches following methods adapted from Payn et al. (2005). First, we plotted $S_{w\text{-}add\text{-}dyn}$ against total NO_3-N concentration and fit a linear regression along with 95% confidence intervals to these data. Next, we back extrapolated the linear regression to 0 total NO_3-N (the same concentration referred to as the negative ambient NO_3-N concentration in Payn et al. 2005) to estimate $S_{w\text{-}amb}$. From these $S_{w\text{-}amb}$ estimates, we calculated ambient areal uptake (U_{amb}) and uptake velocity ($V_{f\text{-}amb}$) using (Eqs. 14 and 15):

$$U_{amb} = Q \times [NO_3\text{-}N_{amb}]/S_{w\text{-}amb} \times w \qquad (14)$$

$$V_{f\text{-}amb} = U_{amb}/[NO_3\text{-}N_{amb}] \qquad (15)$$

where U_{amb} is ambient areal uptake rate ($M \times L^{-2} \times T^{-1}$), $[NO_3\text{-}N_{amb}]$ is the ambient stream NO_3-N concentration ($M \times L^{-3}$) (i.e., background $[NO_3\text{-}N]$ without the influence of nutrient addition), $S_{w\text{-}amb}$ is the ambient uptake length (L), and $V_{f\text{-}amb}$ is the ambient uptake velocity ($L \times T^{-1}$).

Total nutrient areal uptake rates and uptake velocities to determine stream uptake kinetics—We calculated total nutrient uptake (U_{tot}) values for the plateau, BTC-integrated, and dynamic TASCC approaches by combining ambient and added nutrient spiraling values (Eq. 16–18):

$$U_{tot\text{-}plat} = U_{amb} + U_{add\text{-}plat} \qquad (16)$$

$$U_{tot\text{-}int} = U_{amb} + U_{add\text{-}int} \qquad (17)$$

$$U_{tot\text{-}dyn} = U_{amb} + U_{add\text{-}dyn} \qquad (18)$$

where $U_{tot\text{-}plat}$ is total areal uptake rate ($M \times L^{-2} \times T^{-1}$) calculated using the plateau approach, $U_{add\text{-}plat}$ is the added nutrient areal uptake ($M \times L^{-2} \times T^{-1}$) calculated using the plateau approach, $U_{tot\text{-}int}$ is the total areal uptake ($M \times L^{-2} \times T^{-1}$) calculated using the BTC-integrated approach, $U_{add\text{-}int}$ is the added nutrient areal uptake ($M \times L^{-2} \times T^{-1}$) calculated using the BTC-integrated approach, $U_{tot\text{-}dyn}$ is the total areal uptake ($M \times L^{-2} \times T^{-1}$) for each grab sample across the BTC calculated using the dynamic TASCC approach, and $U_{add\text{-}dyn}$ is the added nutrient areal uptake ($M \times L^{-2} \times T^{-1}$) for each grab sample across the BTC calculated using the dynamic TASCC approach (note that $U_{add\text{-}dyn\text{-}MB}$ or $U_{add\text{-}dyn\text{-}TT}$ can be substituted in place of $U_{add\text{-}dyn}$ in Eq. 18 to calculate $U_{tot\text{-}dyn\text{-}MB}$ and $U_{tot\text{-}dyn\text{-}TT}$). Total uptake velocities ($V_{f\text{-}tot}$) were calculated as (Eq. 19–21):

$$V_{f\text{-}tot\text{-}plat} = U_{tot\text{-}plat}/[NO_3\text{-}N_{tot\text{-}plat}] \qquad (19)$$

$$V_{f\text{-}tot\text{-}int} = U_{tot\text{-}int}/[NO_3\text{-}N_{tot\text{-}int}] \qquad (20)$$

$$V_{f\text{-}tot\text{-}dyn} = U_{tot\text{-}dyn}/[NO_3\text{-}N_{tot\text{-}dyn}] \qquad (21)$$

where $V_{f\text{-}tot\text{-}plat}$ is the total uptake velocity ($L \times T^{-1}$) calculated with the plateau approach, $[NO_3\text{-}N_{tot\text{-}plat}]$ is the geometric mean of total (i.e., not background corrected) NO_3-N concentrations ($M \times L^{-3}$) from 12 longitudinal grab samples collected along the stream reach during constant-rate plateau conditions, $V_{f\text{-}tot\text{-}int}$ is the total uptake velocity ($L \times T^{-1}$) calculated with the BTC-integrated approach, $[NO_3\text{-}N_{tot\text{-}int}]$ is the geometric mean of total (i.e., not background corrected) observed and conservative NO_3-N concentration ($M \times L^{-3}$) integrated across the BTC, $V_{f\text{-}tot\text{-}dyn}$ is the total dynamic uptake velocity ($L \times T^{-1}$) for each grab sample across the BTC calculated with the dynamic TASCC approach, and $[NO_3\text{-}N_{tot\text{-}dyn}]$ is the geometric mean of total observed and conservative NO_3-N concentration ($M \times L^{-3}$) in the grab sample of interest. The $[NO_3\text{-}N_{tot\text{-}int}]$ and $[NO_3\text{-}N_{tot\text{-}dyn}]$ values were calculated as (Eq. 22–23):

Where $[NO_3\text{-}N_{tot\text{-}obs}]$ is the total (i.e., not background corrected) NO_3-N observed in a grab sample. The use of total

nutrient spiraling values is important because if one seeks to fit kinetic models (e.g., M-M equation) to areal uptake (or uptake velocity sensu Newbold et al. 2006) versus nutrient concentration curves, it is total N concentration and total uptake rate or uptake velocity that must be used rather than those determined simply from added nutrient. In this case study, we fit the M-M model along with 95% confidence intervals (SigmaPlot, SPSS) to our $U_{tot\text{-}dyn}$ and $V_{f\text{-}tot\text{-}dyn}$ data and determined U_{max} and K_m values using Eq. 24–25):

$$U = \frac{U_{max} * C}{K_m + C} \qquad (24)$$

$$V_f = \frac{U_{max}}{K_m + C} \qquad (25)$$

where C is nutrient concentration, Eq. 24 is the M-M equation, and Eq. 25 is the M-M equation where V_f has been substituted for U (e.g., Earl et al. 2006). Also we included U_{amb} and $V_{f\text{-}amb}$ in our M-M parameterizations to constrain the models to ambient spiraling. We provide 95% confidence intervals to assess both the similarity among approaches and the goodness of fit of M-M parameters. While we used the M-M model in this case study, other kinetic models may apply in different stream systems.

Assessment

Figure 3 displays NO_3-N and Cl BTCs and changing NO_3-N:Cl ratio sampled at the base of the reach, along with the NO_3-N:Cl injectate ratio released at the head of the reach for the Middle Fork nutrient slug. NO_3-N concentrations varied from 18–340 μg L^{-1} and Cl ranged between 374–3250 μg L^{-1} (Fig. 3). The ratio of NO_3-N:Cl varied from 0.05–0.11 and approached the injectate ratio of 0.15 at the peak of the BTC. This changing ratio represents differential transport of NO_3-N relative to Cl, and higher ratios indicate more conservative NO_3-N transport (i.e., near BTC peak) compared with lower ratios that demonstrate stronger NO_3-N uptake (i.e., BTC tails). Furthermore, the changing ratio across the BTC allows calculation of dynamic uptake metrics as a function of concentration using TASCC.

Figure 4A,B displays $S_{w\text{-}add\text{-}dyn}$, $S_{w\text{-}add\text{-}int}$, and $S_{w\text{-}add\text{-}plat}$ plotted against the geometric mean of total (i.e., not background corrected) NO_3-N concentrations for Beehive and Middle Fork. The magnitude of $S_{w\text{-}add\text{-}dyn}$ increased linearly with greater NO_3-

$$[NO_3\text{-}N_{tot\text{-}int}] = \sqrt{\frac{Q\int_0^t [NO_3\text{-}N_{tot\text{-}obs}](t)\,dt}{\int_0^t Q(t)\,dt} * \frac{Q\int_0^t ([NO_3\text{-}N_{cons}] + [NO_3\text{-}N_{amb}])(t)\,dt}{\int_0^t Q(t)\,dt}} \qquad (22)$$

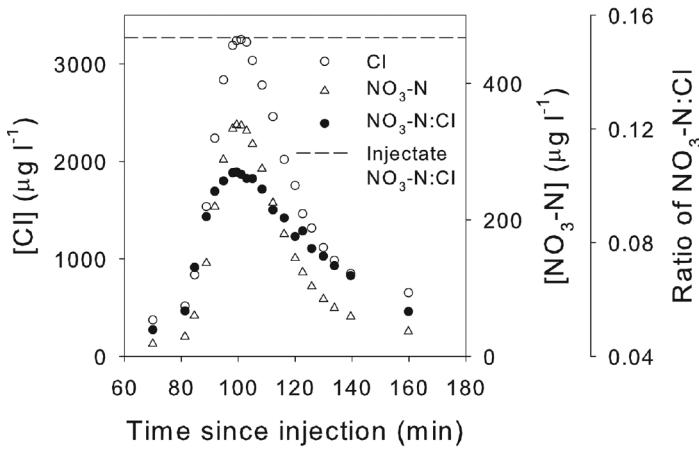$$[NO_3\text{-}N_{tot\text{-}dyn}] = \sqrt{[NO_3\text{-}N_{tot\text{-}obs}] * ([NO_3\text{-}N_{cons}] + [NO_3\text{-}N_{amb}])} \qquad (23)$$

Fig. 3. Cl and NO_3-N BTCs sampled at the base of the Middle Fork slug experiment, along with the changing ratio of NO_3-N:Cl sampled at the base of the reach and the injectate ratio added at the head of the reach. The injectate was added instantaneously at the head of the reach at time 0; however, we show the dashed line to provide context for interpreting the changing ratio at the base of the reach.

N concentrations (Fig. 4A,B). Coefficients of determination (r^2) values derived from linear regression of $S_{w-add-dyn}$ versus nutrient concentration were 0.69 at Beehive and 0.97 at Middle Fork (Fig. 4A,B). $S_{w-add-plat}$ and $S_{w-add-int}$ values also increased linearly with concentration and trended along the $S_{w-add-dyn}$ curves (Fig. 4A,B). $S_{w-add-plat}$ values at Beehive were 2534 and 4140 m with corresponding [NO_3-$N_{tot-plat}$] values of 23 and 103 μg L^{-1}, while Middle Fork $S_{w-add-plat}$ was 3483 m at a [NO_3-$N_{tot-plat}$] of 516 μg L^{-1} (Table 2). $S_{w-add-int}$ at Beehive was 2735 m at a [NO_3-$N_{tot-int}$] of 50 μg L^{-1}, and at Middle Fork $S_{w-add-int}$ was 2325 m at a [NO_3-$N_{tot-int}$] of 214 μg L^{-1} (Table 3). We added 95% confidence intervals to the $S_{w-add-dyn}$ linear regressions to determine how the $S_{w-add-int}$ and $S_{w-add-plat}$ values compared with the dynamic TASCC data. At Beehive, one of the two $S_{w-add-plat}$ values and the $S_{w-add-int}$ value fell within the $S_{w-add-dyn}$ 95% confidence intervals, while one of the $S_{w-add-plat}$ values fell just beyond the confidence band (Fig. 4A). At Middle Fork $S_{w-add-int}$ and $S_{w-add-plat}$ plotted at the limits of the confidence intervals (Fig. 4B).

Regressions of $S_{w-add-dyn}$ and total NO_3-N concentration to estimate S_{w-amb} were based on 14 and 21 data points at Beehive and Middle Fork, respectively (Fig. 4A,B). Results at Beehive (r^2 = 0.69, P = 0.0003) and Middle Fork (r^2 = 0.97, P < 0.0001) displayed linear relationships between $S_{w-add-dyn}$ and concentration as predicted by M-M kinetics (Fig. 4). Ambient spiraling metrics derived from these models differed predictably from BTC-integrated values (Table 3). $S_{w-add-int}$ values were 2.3–2.8 times longer, $V_{f-tot-int}$ measures were 1.75–2.3 times lower, and $U_{tot-int}$ metrics 2.7–10.9 times greater than ambient parameters with enrichments of 5–25 times background concentrations during slug additions (Table 3).

Figure 4C,D shows $V_{f-tot-dyn}$, $V_{f-tot-int}$, and $V_{f-tot-plat}$ plotted against the geometric mean of total (i.e., not background corrected) NO_3-N concentrations for Beehive and Middle Fork.

$V_{f-tot-dyn}$ values declined hyperbolically with increased NO_3-N at both study sites, consistent with M-M kinetic relationships (Fig. 4C,D). At Beehive $V_{f-tot-dyn}$ varied from 0.67–6.55 mm min^{-1} over a 2–117 μg L^{-1} nutrient concentration range (Fig. 4C), whereas Middle Fork $V_{f-tot-dyn}$ values ranged from 0.65–1.78 mm min^{-1} over a 79–454 μg L^{-1} concentration range (Fig. 4D). Results from TASCC, BTC-integrated, and plateau approaches agreed closely across experiments. $V_{f-tot-plat}$ for Beehive (1.2 and 0.7 mm min^{-1}) and Middle Fork (0.6 mm min^{-1}) plotted within the $V_{f-tot-dyn}$ 95% confidence intervals derived from TASCC and were indistinguishable from $V_{f-tot-dyn}$ data (Fig. 4C,D).

Figure 4E,F displays $U_{tot-dyn}$, $U_{tot-int}$, and $U_{tot-plat}$ plotted against the geometric mean of total NO_3-N concentrations for Beehive and Middle Fork. $U_{tot-dyn}$ values increased hyperbolically with increased NO_3-N at both sites (Fig. 4E,F), again indicative of M-M kinetics. At Beehive $U_{tot-dyn}$ ranged from 17–108 μg m^{-2} min^{-1} over a 2–117 μg L^{-1} nutrient concentration range (Fig. 4E), whereas Middle Fork $U_{tot-dyn}$ values ranged from 141–302 μg m^{-2} min^{-1} over a 79–454 μg L^{-1} concentration range (Fig. 4F). Results between the different approaches agreed well and BTC-integrated and plateau values plotted within or at the limit of $U_{tot-dyn}$ 95% confidence intervals developed with TASCC (Fig. 4E,F). M-M model parameter values determined from nonlinear regression were derived from strong model fits (r^2 = 0.76, P < 0.0001 at Beehive; r^2 = 0.98, P < 0.0001 at Middle Fork, Fig. 4E,F) with reasonable values. U_{max} was 19.8 and 4.3 times greater than U_{amb} in Beehive and Middle Fork, respectively, while K_m was 12 and 3.5 times greater than ambient NO_3-N (Table 3). The dynamic TASCC ($U_{tot-dyn}$) and TASCC mass-balance ($U_{tot-dyn-MB}$) approaches yielded very similar assessment of in-stream nutrient uptake (Fig. 5). Linear regression of these two approaches demonstrated the two were indistinguishable with r^2 of >0.999 and P value <0.0001 (Fig. 5).

Figure 6A shows $V_{f-tot-dyn}$ and $V_{f-tot-dyn-TT}$ plotted against total nutrient concentration for the Middle Fork site. These comparisons use the same data set analyzed with two approaches, however, it may appear that the number of values for each method is different because some points near the BTC peak have been obscured from view. While the $V_{f-tot-dyn}$ data trend along the same trajectory for rising and falling limbs (i.e., lack of hysteresis), the $V_{f-tot-dyn-TT}$ values are different for comparable NO_3-N concentrations between the two limbs of the BTC and show stronger uptake on the rising limb (Fig. 6A). Similar results are demonstrated for the $U_{tot-dyn}$ and $U_{tot-dyn-TT}$ values plotted against total nutrient concentration (Fig. 6B). Specifically, while the $U_{tot-dyn}$ values do not indicate any hysteretic behavior, the $U_{tot-dyn-TT}$ values are different at comparable concentrations (Fig. 6B). However, the hysteretic behavior displayed in the travel time approach values is not present in the $S_{w-add-dyn}$ data (Fig. 4A,B) (a metric that is time independent) or the N:Cl data from which the $S_{w-add-dyn}$ values are directly calculated.
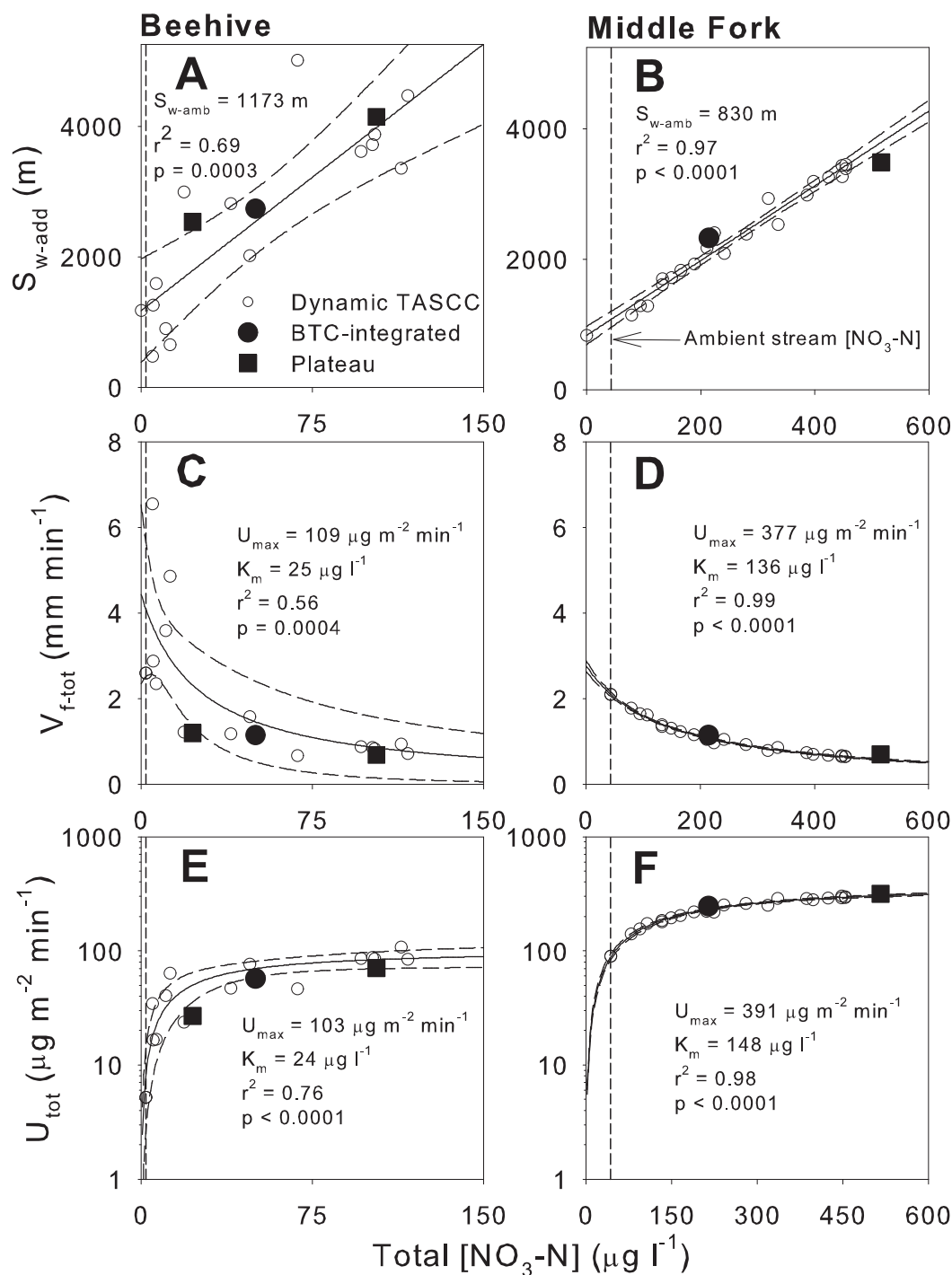
Fig. 4. (A–B) Added nutrient uptake length ($S_{w\text{-}add}$) calculated using the dynamic TASCC ($S_{w\text{-}add\text{-}dyn}$), BTC-integrated ($S_{w\text{-}add\text{-}int}$), and plateau ($S_{w\text{-}add\text{-}plat}$) approaches plotted against the geometric mean of total (i.e., not background corrected) nutrient concentration for Beehive (A) and Middle Fork (B), along with ambient uptake length ($S_{w\text{-}amb}$) and linear regression r^2 and p values (all regressions shown as solid lines and 95% confidence intervals shown as dashed). (C–D) Total uptake velocity ($V_{f\text{-}tot}$) calculated using the dynamic TASCC ($V_{f\text{-}tot\text{-}dyn}$), BTC-integrated ($V_{f\text{-}tot\text{-}int}$), and plateau ($V_{f\text{-}tot\text{-}plat}$) approaches plotted against the geometric mean of total nutrient concentration for Beehive (C) and Middle Fork (D) along with hyperbolic decay model r^2 and p values, and Michaelis-Menten (M-M) parameters maximum uptake (U_{max}) and half-saturation constant (K_m) values. (E–F) Total areal uptake rate (U_{tot}) calculated using the dynamic TASCC ($U_{tot\text{-}dyn}$), BTC-integrated ($U_{tot\text{-}int}$), and plateau ($U_{tot\text{-}plat}$) approaches plotted against the geometric mean of total nutrient concentration for Beehive (E) and Middle Fork (F) along with M-M model fits and 95% confidence intervals, model fit r^2 and p values, and U_{max} and K_m values. Note we performed two constant rate additions at Beehive.

Table 2. Results from constant-rate tracer addition experiments for the Beehive and Middle Fork sites. $S_{w\text{-}add\text{-}plat}$, $V_{f\text{-}tot\text{-}plat}$, and $U_{tot\text{-}plat}$ were calculated using the plateau approach. $[NO_3\text{-}N_{tot\text{-}plat}]$ is the geometric mean of total (i.e., not background corrected) observed NO_3-N plateau concentrations of longitudinal grab samples collected along the stream reach.

Site	Date	$[NO_3\text{-}N_{tot\text{-}plat}]$ (µg L^{-1})	$S_{w\text{-}add\text{-}plat}$ (m)	$V_{f\text{-}tot\text{-}plat}$ (mm min^{-1})	$U_{tot\text{-}plat}$ (µg m^{-2} min^{-1})
Beehive	30-Jul-08	23	2534	1.2	27
Beehive	30-Jul-08	103	4140	0.7	71
Middle Fork	22-Aug-07	516	3483	0.6	316

Table 3. Ambient* and nutrient slug BTC-integrated[†] measures of spiraling metrics, associated concentration of NO_3-N[‡], and derived Michaelis-Menten parameter estimates at Beehive and Middle Fork sites.

	Beehive	Middle fork
Ambient		
$S_{w\text{-}amb}$ (m)	1173	830
$V_{f\text{-}amb}$ (mm min^{-1})	2.6	2.1
U_{amb} (µg m^2 min^{-1})	5.2	90
$NO_3\text{-}N_{amb}$ (µg L^{-1})	2	43
BTC-integrated (enriched)		
$S_{w\text{-}add\text{-}int}$ (m)	2735	2325
$V_{f\text{-}tot\text{-}int}$ (mm min^{-1})	1.14	1.15
$U_{tot\text{-}int}$ (µg m^2 min^{-1})	57	247
$NO_3\text{-}N_{tot\text{-}int}$ (µg L^{-1})	50	214
Michaelis-Menten		
K_m (µg L^{-1})	24	148
U_{max} (µg m^2 min^{-1})	103	391

*Ambient metrics were derived using the Payn et al. (2005) approach constrained with dynamic TASCC data.

[†]BTC-integrated nutrient slug enrichment metrics were calculated using the BTC-integrated approach.

[‡]$NO_3\text{-}N_{amb}$ is the ambient nutrient concentration (i.e., concentration without influence of nutrient addition), and $NO_3\text{-}N_{tot\text{-}int}$ is the geometric mean of BTC-integrated total (i.e., not background corrected) observed and conservative NO_3-N concentrations.
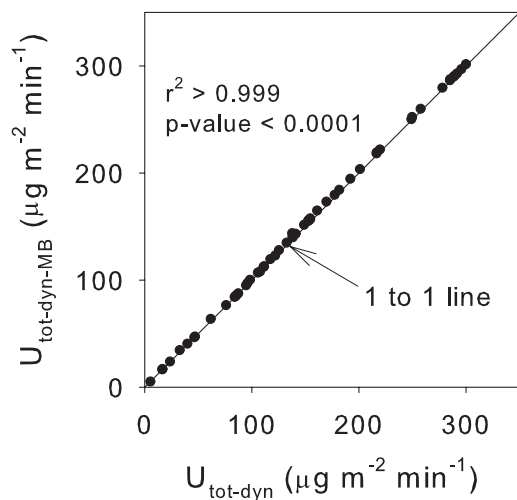

Fig. 5. Linear regression comparing total areal uptake (U_{tot}) calculations using an exponential decay model (i.e., $U_{tot\text{-}dyn}$ calculated using $k_{w\text{-}dyn}$) and a mass balance approach ($U_{tot\text{-}dyn\text{-}MB}$).
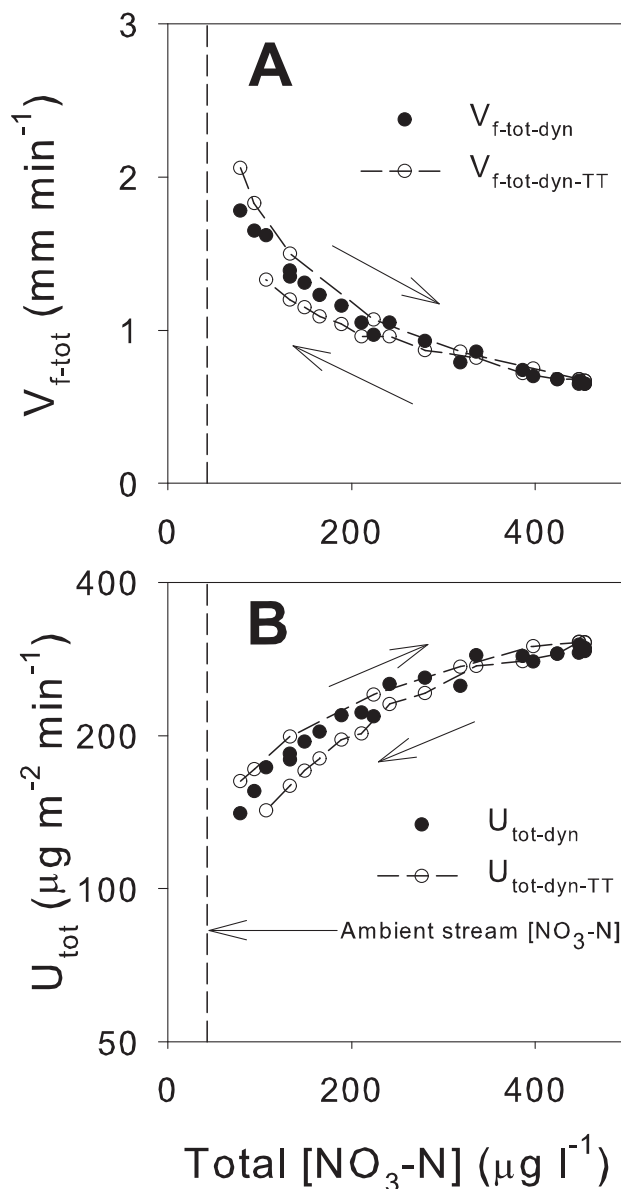

Fig. 6. (A) Total dynamic uptake velocity ($V_{f\text{-}tot\text{-}dyn}$) and total dynamic uptake velocity calculated with the variable travel time approach ($V_{f\text{-}tot\text{-}dyn\text{-}TT}$) plotted against total dynamic nutrient concentration, and (B) total dynamic areal uptake rate ($U_{tot\text{-}dyn}$) and total dynamic areal uptake rate calculated with the variable travel time approach ($U_{tot\text{-}dyn\text{-}TT}$) plotted against total dynamic nutrient concentration. Arrows indicate direction of hysteresis in the variable travel time metrics.

Discussion

In this article, we present, outline, and demonstrate a new approach (TASCC) for rapid assessment of nutrient uptake kinetics and spiraling curve characterization. We compare the results generated using TASCC with those from BTC-integrated and plateau approaches. These comparisons demonstrated that BTC-integrated and plateau approach values typically fell within TASCC 95% confidence intervals (Fig. 4), indicating no significant differences between spiraling metrics generated using these different approaches. However, we seek to highlight the advantages of the TASCC approach for rapid characterization of spiraling response curves and parameterization of uptake kinetic models. In addition to being rapid, relatively easy, and cost effective, the TASCC method produces greater data density and more continuous spiraling response curves than previous approaches (e.g., successive plateau experiments). This is important because inadequate spiraling response curve characterization, and incomplete assessment of the influence of concentration on nutrient retention (i.e., uptake) and export have both been noted as problematic (Dodds et al. 2002; Mulholland et al. 2008). Also, increased data density using the TASCC approach improves extrapolations to estimate ambient spiraling metrics from nutrient addition experiments (e.g., Payn et al. 2005). The TASCC approach also provides assessment of stream reach proximities to saturation (i.e., saturation response types [SRTs] Earl et al. 2006), which is important for understanding how streams might respond to increased nutrient load (i.e., buffering potential). Not only can these nutrient spiraling metrics be quantified in small streams typically studied in plateau experiments, but TASCC can also be applied across the continuum of stream sizes (i.e., small to large). We suggest TASCC is a cost-effective, rapid, and relatively easy technique that provides: 1) improved confidence in estimates of ambient-spiraling metrics determined from nutrient addition experiments; 2) enhanced characterization of spiraling response curves and parameterization of kinetic models; 3) accordingly better assessment of stream saturation state and intersystem comparison; and 4) applicability to large river systems where obtaining constant-rate plateau conditions is impractical.

Due to the high cost associated with directly measuring ambient nutrient spiraling using isotopically labeled tracers (e.g., ^{15}N) and the health concerns associated with using radiotracers (e.g., ^{32}P, ^{33}P), other methods have been developed to estimate ambient spiraling parameters from less expensive and benign unlabeled nutrient addition experiments (e.g., Dodds et al. 2002; Payn et al., 2005). These methods capitalize upon relationships between nutrient concentration and spiraling (i.e., uptake) to extrapolate to concentrations that represent ambient spiraling. Typically, these spiraling curve relationships have been characterized using constant-rate tracer additions (i.e., plateau approach) performed at various added nutrient concentrations (Dodds et al. 2002; Payn et al. 2005;

Earl et al. 2007). However, adequate characterization of these curves using the plateau approach has proven challenging, partially due to the large amount of time and effort involved in each plateau experiment. Conversely, the TASCC approach provides a method for rapid characterization of these curves with a single tracer addition. Linear regressions of $S_{w\text{-}add\text{-}dyn}$ and nutrient concentration that we used to estimate $S_{w\text{-}amb}$ were developed from single tracer additions at each study site, and to the best of our knowledge, these are the first spiraling regressions to have this type of data density within a stream reach. This increased data density should help improve extrapolations to estimate ambient spiraling parameters, which is a useful approach given the high costs and health concerns associated with measuring ambient spiraling using stable isotope or radio labeled tracers.

Another benefit of the TASCC approach is that total spiraling parameters can be quantified through the combination of ambient and added nutrient spiraling metrics. This is important because to correctly parameterize kinetic models, it is critical that total spiraling values be used. This is demonstrated in conceptual Figure 2D, which shows uptake concentration curves for total (U_{tot}) and added nutrient (U_{add}). Because spiraling measured during a nutrient addition experiment is that of added nutrient, the measured uptake at zero-added nutrient concentration (i.e., ambient concentration with no influence of added nutrient) will appear to be 0 µg m^{-2} min^{-1} (Fig. 2D). However, this neglects to recognize that U_{add} occurs in addition to U_{amb} also occurring in the stream reach (Fig. 2D). For this reason, if kinetic models are parameterized using U_{add} instead of U_{tot} data, the parameter values will be incorrect.

An improved understanding of the relationship between nutrient spiraling and concentration has been noted as important to improve nutrient export models (Mulholland et al. 2008), but is also useful to assess stream proximity to saturation (e.g., Earl et al. 2006) and to increase basic understanding of stream solute transport. Because TASCC provides for spiraling curve characterization from ambient to saturation, we were able to quantify relationships between $V_{f\text{-}tot}$, U_{tot}, and concentration. Because V_f is indicative of nutrient use efficiency, these curves represent the impact increased nutrient load has on use (i.e., uptake) relative to concentration. In our study, $V_{f\text{-}tot\text{-}dyn}$ decreased far less over a larger concentration range at Middle Fork and suggests this reach may have greater resiliency to increased nutrient load relative to the Beehive reach (Fig. 2C,D). These types of dynamics would be difficult to detect if analysis had relied solely on plateau approach values; which highlights the utility of characterizing the entire spiraling curve. Further, the $U_{tot\text{-}dyn}$ data allow for elucidation of dynamics not evident in less dense data sets (i.e., plateau approach data sets), and improve confidence in kinetic model parameter value estimates through increased uptake data density. The ability to parameterize kinetic models (e.g., M-M model U_{max} and K_m) is important because these parameter values, interpreted in conjunction with ambient spiraling metrics

(e.g., $V_{f\text{-}amb}$ and U_{amb}) also developed with the TASCC method, could aid in stream assessment and inter-stream comparisons. Furthermore, characterization of spiraling from ambient to saturation elucidates stream reach capacity to increase uptake in response to increased loading and proximity to saturation.

None of our dynamic spiraling versus nutrient concentration curves, except for those calculated using the variable travel time approach, demonstrated any time-dependent uptake (evident as hysteresis loops in spiraling curve relationships, Figs. 4 and 6). Lack of hysteretic behavior in the $S_{w\text{-}add\text{-}dyn}$ (a time independent metric) versus [Cl] or nutrient concentration plots, and lack of hysteresis in the raw N:Cl data suggest that the leading edge and tail of the slug BTC elicited comparable uptake responses. We believe that the variable travel time approach forces hysteresis in the $V_{f\text{-}tot\text{-}dyn\text{-}TT}$ and $U_{tot\text{-}dyn\text{-}TT}$ spiraling curves and in this manner is not the preferred approach for calculating dynamic spiraling metrics. Furthermore, in nearly two-dozen tracer addition experiments across a range of stream systems, we have not seen any evidence of hysteretic behavior (Covino et al. 2010; McNamara et al. in prep.). Analysis of the changing NO_3-N:Cl ratio, which is indicative of uptake and biologically active tracer transport relative to conservative tracer transport, as a function of [Cl] or nutrient concentration in these data sets has not indicated any effect of travel time on nutrient uptake and/or spiraling.

However, certain locations (stream reaches) or time periods could demonstrate variability in spiraling metrics between BTC rising and falling limbs, particularly in systems near saturation prior to nutrient addition or with two (or more) very distinct compartments. We suggest that use of the TASCC approach should reveal times of hysteresis by quantifying differences in spiraling on the rising and falling limbs of BTCs (as a function of time or history of exposure). These differences would be evident in raw N:Cl data and in the $S_{w\text{-}add\text{-}dyn}$ data and would consistently carry through in the $U_{tot\text{-}dyn}$, $U_{tot\text{-}dyn\text{-}MB}$, and $V_{f\text{-}tot\text{-}dyn}$ calculations. Therefore, the ability to elucidate and quantify any temporal dependencies or history of exposure affects is an additional benefit of the TASCC approach.

Research has just begun to address the issue of measuring nutrient spiraling in larger rivers (e.g., Dodds et al. 2008; Tank et al. 2008), and the TASCC approach builds upon these recent advances by providing a method to fully characterize nutrient spiraling response curves across stream sizes. This is important because nutrient export models need to span stream sizes, account for variable nutrient concentration, and incorporate serial processing to provide more accurate export estimates. In addition, because TASCC is relatively fast and easy, these experiments can be performed at different times of the year to assess how seasonal changes in environmental conditions impact nutrient uptake kinetics, spiraling response curves, and nutrient export. Finally, the TASCC approach is not limited to slug additions only. It may be applied to constant-rate BTCs in the same fashion as slug BTC data, so long as grab samples were/are collected on the rising and falling limbs to and from plateau conditions. Also, TASCC can be applied with other biologically active tracers (e.g., P, NH_4, urea, acetate, etc), which could be particularly useful for quantifying P spiraling curves, given the use of P radioisotopes (^{32}P, ^{33}P) is impractical due to health concerns.

Comments and recommendations

Through our experience with the TASCC approach, we have developed some recommendations that should help improve the quality of data produced using the method. First, in order to characterize spiraling response curves and uptake kinetics, it is important to push the stream to near saturated (or saturated) conditions. This is similar to enzyme kinetic experiments performed in a laboratory where uptake is measured across a range of substrate concentrations from zero substrate to near saturated (or saturated) conditions (e.g., Voet and Voet 1995). Next, the BTC of the tracer addition must be sampled across the entirety of the nutrient concentration range (i.e., across BTC) with substantial resolution to characterize spiraling at all concentrations experienced across the BTC. We have also found that longer stream reach distances, larger grab sample volumes (e.g., 250–1000 mL), and collecting samples from a fixed location in the channel (i.e., sampling through a tube attached to a post driven into the streambed) help to decrease sampling induced variability in spiraling curve data. This is particularly relevant in highly advective systems and/or those with substantial gains and losses to and from groundwater. In terms of hydrology, it is important to measure Q at both the head and base of the stream reach. Conservative tracer released at the head of the reach cannot be used to calculate Q at the base of the reach. This is because conservative tracer mass loss (i.e., hydrologic loss) along the stream length will lead to incorrect overestimates of Q at the base of the reach (this is true for both slug and constant-rate releases) (e.g., Payn et al. 2009). Also we encourage the use of the mass-balance approach for calculating uptake because it is a direct measure of nutrient use across the reach. Mass-balance derived uptake measures can be converted to S_w and V_f values to provide a full suite of spiraling metrics. These considerations should help to improve data quality and facilitate application of the method.

We suggest that the TASCC approach is a useful, inexpensive, and efficient technique to characterize spiraling response curves from ambient to saturation. Specifically this approach provides 1) improved confidence in estimates of ambient spiraling metrics determined from nutrient addition experiments; 2) enhanced characterization of spiraling response curves and parameterization of kinetic models; 3) accordingly better assessment of stream saturation state and inter-system comparison; and 4) applicability to large river systems where obtaining constant-rate plateau conditions is impractical. Future research directions include 1) corroboration of TASCC with stable isotope approaches across systems and biomes; 2) developing improved understanding of the controls over spatially and tem-

porally variable kinetic response curves; and 3) implementing these dynamics in export models to quantify and assess the role of stream networks in modifying downstream transport.

We have demonstrated that BTC-integrated, and plateau approach spiraling values typically fell within dynamic TASCC data 95% confidence intervals, indicating correspondence between these three different approaches. However, we note that ambient, BTC-integrated, and plateau metrics each represent only one value on the greater spiraling characteristic curve. In conclusion, we suggest that nutrient spiraling response curves, ambient spiraling metrics, uptake kinetics from ambient to saturation, and kinetic model parameterization quantified using the TASCC approach should help increase our basic understanding of nutrient spiraling, improve nutrient export models, and aid in stream saturation assessment across the continuum of stream sizes.

References

Barbagelata, A. 1928. Chemical-electrical measurement of water. Proc. Am. Soc. Civil Eng. 54:789-802.

Bernhardt, E. S., G. E. Likens, D. C. Buso, and C. T. Driscoll. 2003. In-stream uptake dampens effects of major forest disturbance on watershed nitrogen export. Proc. Nat. Acad. Sci. U.S.A. 100:10304-10308 [doi:10.1073/pnas.1233676100].

Covino, T., B. L. McGlynn, and M. Baker. In press. 2010. Separating physical and biological nutrient retention and quantifying uptake kinetics from ambient to saturation in successive mountain stream reaches. J. Geophys. Res. Biogeosci. [doi:10.1029/2009JG001263].

Dodds, W. K., and others. 2002. N uptake as a function of concentration in streams. J. North Am. Benthol. Soc. 21:206-220 [doi:10.2307/1468410].

———, and others. 2008. Nitrogen cycling and metabolism in the thalweg of a prairie river. J. Geophys. Res. Biogeosci. 113:G04029 [doi:10.1029/2008JG000696].

Earl, S. R., H. M. Valett, and J. R. Webster. 2006. Nitrogen saturation in stream ecosystems. Ecology 87:3140-3151 [doi:10.1890/0012-9658(2006)87[3140:NSISE]2.0.CO;2].

———, H. M. Valett, and J. R. Webster. 2007. Nitrogen spiraling in streams: Comparisons between stable isotope tracer and nutrient addition experiments. Limnol. Oceanogr. 52:1718-1723.

Gardner, K. K., and B. L. McGlynn. 2009. Seasonality in spatial variability and influence of land use/land cover and watershed characteristics on streamwater nitrate concentrations in a developing watershed in the rocky mountain west. Wat. Resources Res. 45 [doi:10.1029/2008WR007029].

Hart, B. T., P. Freeman, and I. D. McKelvie. 1992. Whole-stream phosphorus release studies—variation in uptake length with initial phosphorus concentration. Hydrobiologia 235:573-584 [doi:10.1007/BF00026245].

McNab, W. H. 1996. Ecological Subregions of the United States. U.S. Department of Agriculture, Forest Service. <http://www.fs.fed.Us/land/pubs/ecoregions/>.

Mulholland, P. J., A. D. Steinman, and J. W. Elwood. 1990. Measurement of phosphorus uptake length in streams—comparison of radiotracer and stable po4 releases. Can. J. Fish. Aquat. Sci. 47:2351-2357 [doi:10.1139/f90-261].

———, and others. 2002. Can uptake length in streams be determined by nutrient addition experiments? Results from an interbiome comparison study. J. North Amer. Benthol. Soc. 21:544-560 [doi:10.2307/1468429].

———, and others. 2008. Stream denitrification across biomes and its response to anthropogenic nitrate loading. Nature 452:202-205 [doi:10.1038/nature06686].

Newbold, J. D., J. W. Elwood, R. V. Oneill, and W. Vanwinkle. 1981. Measuring nutrient spiralling in streams. Can. J. Fish. Aquat. Sci. 38:860-863 [doi:10.1139/f81-114].

———, J. W. Elwood, R. V. Oneill, and A. L. Sheldon. 1983. Phosphorus dynamics in a woodland stream ecosystem - a study of nutrient spiralling. Ecology 64:1249-1265 [doi:10.2307/1937833].

———, and others. 2006. Uptake of nutrients and organic C in streams in New York City drinking-water-supply watersheds. J. North Am. Benthol. Soc. 25:998-1017.

O'Brien, J. M., W. K. Dodds, K. C. Wilson, J. N. Murdock, and J. Eichmiller. 2007. The saturation of N cycling in central plains streams: N-15 experiments across a broad gradient of nitrate concentrations. Biogeochemistry 84:31-49 [doi:10.1007/s10533-007-9073-7].

Payn, R. A., J. R. Webster, P. J. Mulholland, H. M. Valett, and W. K. Dodds. 2005. Estimation of stream nutrient uptake from nutrient addition experiments. Limnol. Oceanogr. Methods 3:174-182.

———, M. N. Gooseff, B. L. McGlynn, K. E. Bencala, and S. M. Wondzell. 2009. Channel water balance and exchange with subsurface flow along a mountain headwater stream in Montana, United States. Water Resour. Res. 45, W11427 [doi:10.1029/2008WR007644].

Rabalais, N. N., R. E. Turner, R. J. Diaz, and D. Justic. 2009. Global change and eutrophication of coastal waters. ICES J. Mar. Sci. 66:1528-1537 [doi:10.1093/icesjms/fsp047].

Royer, T. V., J. L. Tank, and M. B. David. 2004. Transport and fate of nitrate in headwater agricultural streams in Illinois. J. Environ. Qual. 33:1296-1304 [doi:10.2134/jeq2004.1296].

Ruggiero, A., A. G. Solimini, M. Anello, A. Romano, M. De Cicco, and G. Carchini. 2006. Nitrogen and phosphorus retention in a human altered stream. Taylor & Francis.

Stream Solute Workshop. 1990. Concepts and methods for assessing solute dynamics in stream ecosystems. J. North Am. Benthol. Soc. 9:95-119 [doi:10.2307/1467445].

Tank, J. L., E. J. Rosi-Marshall, M. A. Baker, and R. O. Hall. 2008. Are rivers just big streams? A pulse method to quantify nitrogen demand in a large river. Ecology 89:2935-2945 [doi:10.1890/07-1315.1].

Triska, F. J., V. C. Kennedy, R. J. Avanzino, G. W. Zellweger, and K. E. Bencala. 1989. Retention and transport of nutrients in a 3rd-order stream in northwestern California—

hyporheic processes. Ecology 70:1893-1905 [doi:10.2307/1938120].

Turner, R. E., and N. N. Rabalais. 2003. Linking landscape and water quality in the Mississippi River basin for 200 years. Bioscience 53:563-572 [doi:10.1641/0006-3568(2003)053 [0563:LLAWQI]2.0.CO;2].

Vitousek, P. M., J. D. Aber, R. W. Howarth, G. E. Likens, P. A. Matson, D. W. Schindler, W. H. Schlesinger, and D. G. Tilman. 1997. Human alteration of the global nitrogen cycle: Sources and consequences. Ecol. Appl. 7:737-750.

Voet, D., and J. Voet. 1995. Biochemistry, 2nd ed. Wiley.

Wallace, J. B., J. R. Webster, and W. R. Woodall. 1977. Role of filter feeders in flowing waters. Arch. Hydrobiol. 79:506-532.

Webster, J. R. 1975. Analysis of potassium and calcium dynamics in stream ecosystems on three southern appalachian watersheds of contrasting vegetation. Doctoral dissertation, University of Georgia.

———, and B. C. Patten. 1979. Effects of watershed perturbation on stream potassium and calcium dynamics. Ecol. Monogr. 49:51-72 [doi:10.2307/1942572].